


RESEARCH

Open Access



Parametric modeling and model order reduction for (electro-)thermal analysis of nanoelectronic structures

Lihong Feng¹, Yao Yue^{1*} , Nicodemus Banagaaya¹, Peter Meuris², Wim Schoenmaker² and Peter Benner¹

*Correspondence:

yue@mpi-magdeburg.mpg.de

¹Max Planck Institute for Dynamics of Complex Technical Systems, Sandtorstr. 1, Magdeburg, 39106, Germany

Full list of author information is available at the end of the article

Abstract

In this work, we discuss the parametric modeling for the (electro)-thermal analysis of components of nanoelectronic structures and automatic model order reduction of the consequent parametric models. Given the system matrices at different values of the parameters, we introduce a simple method of extracting system matrices which are independent of the parameters, so that parametric models of a class of linear parametric problems can be constructed. Then the reduced-order models of the large-scale parametric models are automatically obtained using *a posteriori* output error bounds for the reduced-order models. Simulations of both thermal and electro-thermal systems confirm the validity of the proposed methods.

1 Introduction

Parameter variations have become essential in the design of micro- and nano-electronic (-mechanical) systems as well as of coupled electro-thermal problems, since in many analyses such as optimization and uncertainty quantification, modeling and simulation at many values of the parameters are unavoidable. For many design and analysis tools, modeling and simulation need to be done at each instance of the parameter from scratch: given a fixed value of the parameter, say p^* , a certain numerical discretization method, e.g., a finite element method, is used to build a spatially discretized model only valid for p^* , and numerical integration is then performed to get the output response corresponding to p^* . If additional analysis beyond the capability of the aforementioned software is required, the software often can provide only the (conductivity, capacitance) matrices corresponding to certain samples of the parameter, rather than explicit matrix functions that are more convenient for mathematical analysis.

It is desired to derive a single parametric discretized system that is valid for all possible values of the parameters, so that discretization does not have to be implemented anew for each value of interest, which can save much simulation time. In this paper, we propose a simple method of extracting matrix functions that is capable of calculating the matrices corresponding to any parameter value efficiently. Thanks to these matrix functions, the dynamics of the parametric system can be described by a single system of parametric ordinary differential equations (ODEs) or differential-algebraic equations (DAEs).

The approach is in particular suitable for the (electro)-thermal analysis of nanoelectronic structures, as the parameters there often appear in a linear affine form required by this extraction for a parametric model.

Simulating the consequent parametric system is, however, still very time consuming, because of the high dimension of the system. We propose to use parametric model order reduction (PMOR) to compute a reduced-order model (ROM) that is not only of a much lower dimension, but also accurate for all values of the parameters within a specified range. Therefore, using the parametric ROM to replace the full-order model (FOM) in simulation and other analyses like optimization and uncertainty quantification leads to significant speedup and high accuracy. Many PMOR methods have been proposed so far. A survey of PMOR methods can be found in [1]. In this paper, we use a multi-moment-matching PMOR method [2] to construct the reduced-order model. These methods are popular in practical applications since they are easy to implement, need less computations than most of the other methods, and are therefore suitable to reduce high-dimensional ODE/DAE systems that commonly arise in design and analysis of VLSI (very-large-scale integration) circuits. Furthermore, we propose to use an *a posteriori* output error bound [3] to construct the ROM automatically, i.e., the algorithm can build a reduced-order model satisfying a prescribed error tolerance without further specification of algorithmic parameters, e.g., interpolation points and the order of the ROM, which can be automatically determined by the algorithm in an adaptive manner.

The paper is organized as follows. In Section 2, we propose a simple method of extracting the state-space representation of a class of parametric problems. Section 3 reviews the basic idea of PMOR methods and Section 4 describes an algorithm that implements the multi-moment-matching PMOR method adaptively based on an *a posteriori* output error bound for the ROM. Section 5 describes the (electro)-thermal simulation for two test models: a package model and a Power-MOS device model. The parametric modeling and PMOR of these models, especially the extraction of the tensors and PMOR for the one-way nonlinearly coupled dynamical system, are discussed in Section 6. The numerical results are presented in Section 7, and the paper is concluded in Section 8. In all test cases, the matrices are efficiently extracted and the parametric ROMs automatically obtained meet the requirements on accuracy and compactness.

2 Parametric modeling

In this section, we introduce a method for extracting system matrices of a class of parametric problems, so that the parametric representation of the models in state-space form can be derived. Assume that the parametric problem can be generally described by the following partial differential equation,

$$\frac{\partial a(t, z; p)}{\partial t} + \mathcal{L}[a(t, z; p)] = f(t, z; p), \quad t \in [0, T], z \in \Omega, p \in \mathcal{P}, \quad (1)$$

where $\mathcal{L}[\cdot]$ is a linear spatial differential operator, $f(t, z; p)$ is the excitation, $p = (p_1, \dots, p_m)^T$ is a vector of parameters, $\Omega \subseteq \mathbb{R}^d$ ($d = 1, 2, 3$) is the spatial domain and $\mathcal{P} \subseteq \mathbb{R}^m$ is the parameter domain.

In many engineering problems, we are interested in the input-output behavior of system (1). In simulation of integrated circuits, for example, we are often concerned with the currents at the contacts (outputs) rather than inside the circuit when certain voltages are

exerted on the contacts (inputs). In such cases, state-space representation is often used for the spatially discretized system. Using finite-element simulation software, we can usually conduct spacial discretization only at a fixed value p^* of p and obtain the discretized system

$$\begin{aligned}
 E(p^*) \frac{dx(t, p^*)}{dt} &= A(p^*)x(t, p^*) + B(p^*)u(t), \\
 y(t, p^*) &= C(p^*)x(t, p^*) + D(p^*)u(t),
 \end{aligned}
 \tag{2}$$

where only $E(p^*), A(p^*) \in \mathbb{R}^{n \times n}$, $B(p^*) \in \mathbb{R}^{n \times l_1}$, $C(p^*) \in \mathbb{R}^{l_0 \times n}$, and $D(p^*) \in \mathbb{R}^{l_0 \times l_1}$ at the fixed value p^* of p are available. Here, $x \in \mathbb{R}^n$ is the state vector, and $y \in \mathbb{R}^{l_0}$ is the output response. For design purposes, the simulation results at many fixed values of p should be derived and analyzed. If we simply use the software, the discretization must be repeated at many values of p . To avoid repeated discretization in space, and hence to save design time, it is desired that a parametric representation of the model is available.

We will show that if $E(p), A(p), B(p), C(p), D(p)$ are in the form of

$$M(p) = p_1 M_1 + \dots + p_m M_m,
 \tag{3}$$

we can easily compute M_1, \dots, M_m based on the data of $M(p)$ at m fixed values of p (here and below, $M(p)$ stands for any of the matrices $E(p), A(p), B(p), C(p), D(p)$). Hence, the parametric representation of (2) is available, i.e.,

$$\begin{aligned}
 E(p) \frac{dx(t, p)}{dt} &= A(p)x(t, p) + B(p)u(t), \\
 y(t, p) &= C(p)x(t, p) + D(p)u(t).
 \end{aligned}
 \tag{4}$$

The discretized parametric model in (4) not only prevents repeated discretization at all values of p , but also retains the same system order n as the nonparametric system (2) regardless of the number of the parameters. Note that the linear-affine form (3) does not require linear dependence on geometrical and/or physical parameters since p_i may present abstract parameters. It covers a rather broad range of applications since any system of the form

$$M(q) = \phi_1(q)M_1 + \dots + \phi_m(q)M_m,
 \tag{5}$$

where ϕ_i represents an arbitrary scalar function of q , can easily be rewritten into form (3) with the change of parameter $p_i = \phi_i(q)$. The vectors p and q can be of different lengths, e.g., for the package model that will be described in Section 5, we set $p_1 = 1, p_2 = h, p_3 = \frac{1}{h}$, where h is the top layer thickness of the package. Note that any parametric matrix $M(q)$ can be written into the form (5) theoretically since if we denote the (i, j) -th entry of $M(q)$ by $m_{i,j}(q)$, $M(q)$ can be at least expanded as

$$M(q) = \sum_{i=1}^n \sum_{j=1}^n m_{i,j}(q) (e_i e_j^T),$$

where e_i is the i -th column of the $n \times n$ identity matrix. In practice, however, m in (5) should be small enough, e.g., below ten, if PMOR is expected to be efficient on the extracted system. A concise form can often be obtained by physical reasoning provided by engineers. For our test examples in Section 5, $M(h) = M_0 + hM_1 + \frac{1}{h}M_2$ when the thickness parameter h changes, and $M(\sigma) = M_0 + \sigma M_1$ when the conductivity parameter σ changes. However, there are still cases where the space-discretization does not yield a concise affine-linear structure. For such cases, empirical interpolation method [1, 4] is commonly applied to obtain an approximation with an affine structure.

Suppose that m groups of matrices $E(p^{a_i}), A(p^{a_i}), B(p^{a_i}), C(p^{a_i}), D(p^{a_i})$ have been obtained, e.g., by simulation software at m different samples $p^{a_i}, i = 1, \dots, m$. Using the formulation in (3), one can get a group of equations as below,

$$\begin{aligned} p_1^{a_1} M_1 + \dots + p_m^{a_1} M_m &= M(p^{a_1}), \\ \vdots & \\ p_1^{a_m} M_1 + \dots + p_m^{a_m} M_m &= M(p^{a_m}). \end{aligned} \tag{6}$$

The equations above can be re-written as

$$(P_m \otimes I_n) \begin{pmatrix} M_1 \\ \vdots \\ M_m \end{pmatrix} = \begin{pmatrix} M(p^{a_1}) \\ \vdots \\ M(p^{a_m}) \end{pmatrix}, \tag{7}$$

where $I_n \in \mathbb{R}^{n \times n}$ is the identity matrix, and

$$P_m = \begin{pmatrix} p_1^{a_1} & \dots & p_m^{a_1} \\ \vdots & & \vdots \\ p_1^{a_m} & \dots & p_m^{a_m} \end{pmatrix} \in \mathbb{R}^{m \times m}.$$

If p_1, p_2, \dots, p_m are independent parameters, it is possible to select the samples p^{a_i} such that the corresponding $m \times m$ matrix P_m in (7) is nonsingular, since otherwise, one or more parameters can be removed. Under this assumption,

$$\begin{pmatrix} M_1 \\ \vdots \\ M_m \end{pmatrix} = (P_m^{-1} \otimes I_n) \begin{pmatrix} M(p^{a_1}) \\ \vdots \\ M(p^{a_m}) \end{pmatrix},$$

where we use the following property of the Kronecker product: $(U \otimes Q)^{-1} = U^{-1} \otimes Q^{-1}$ for any nonsingular matrices $U \in \mathbb{R}^{n_U \times n_U}$ and $Q \in \mathbb{R}^{n_Q \times n_Q}$ [5]. Finally, the matrices $M_i (i = 1, \dots, m)$ can be easily computed by

$$\begin{aligned} M_1 &= \tilde{p}_{11} M(p^{a_1}) + \dots + \tilde{p}_{1m} M(p^{a_m}), \\ \vdots & \\ M_m &= \tilde{p}_{m1} M(p^{a_1}) + \dots + \tilde{p}_{mm} M(p^{a_m}), \end{aligned} \tag{8}$$

where \tilde{p}_{ij} is the (i, j) -th entry of the matrix P_m^{-1} :

$$P_m^{-1} = \begin{pmatrix} \tilde{p}_{11} & \cdots & \tilde{p}_{1m} \\ \vdots & & \vdots \\ \tilde{p}_{m1} & \cdots & \tilde{p}_{mm} \end{pmatrix}. \tag{9}$$

An important property of the computation above is that it is independent of the large dimension n (typically several thousands or even higher) in linear system solves. To compute all M_i ($M_i = E_i, A_i, B_i, C_i, D_i, i = 1, \dots, m$) in (3) for any large-scale matrices in (2), we need only to invert a small-scale $m \times m$ matrix P_m once (m is typically below ten and equals 2 or 3 in our numerical examples) and conduct scalar-matrix multiplication and matrix addition with the dimension n , all of which are computationally much more efficient than solving (6) with its order mn . Note that the full inverse for such a small matrix can readily be computed, and multiplication with it is somewhat faster than working with the triangular factor and backward/forward solves due to the memory access pattern.

Simulating the system in (4) may still take a lot of time when the dimension n is large, especially when it has to be simulated at many samples of p (like in optimization). In the next section, we propose to use PMOR to construct a parametric reduced-order model, which will replace the original large-scale system in (4) in simulations for speedup. Since the size of the reduced-order model is usually much smaller than n , simulation can be conducted within a much shorter and more reasonable time period.

3 PMOR based on multi-moment-matching

Various PMOR methods have been proposed in the literature, among which the methods based on multi-moment-matching are probably the easiest to implement and the most computationally efficient for many applications, especially for linear systems [2]. The multi-moment-matching PMOR method computes a basis matrix V based on the series expansion of the state vector x in the frequency domain. Under the zero initial condition, the frequency domain description for system (4) is

$$\begin{aligned} (sE(p) - A(p))x(s, p) &= B(p)u(s), \\ y(s, p) &= C(p)x(s, p) + D(p)u(s), \end{aligned} \tag{10}$$

where we assume that the matrix pencil $(A(p), E(p))$ is regular for any p value, i.e., there exists $\lambda_{p,0}$ such that $\lambda_{p,0}E(p) - A(p)$ is nonsingular. Given expansion points $p^0 = [p_1^0, \dots, p_m^0]$, and s_0 , $x(s, p)$ in (10) can be expanded as

$$\begin{aligned} x(s, p) &= [I - (\sigma_1 G_1 + \cdots + \sigma_m G_m + \sigma_{m+1} G_{m+1} + \cdots + \sigma_{2m} G_{2m})]^{-1} B_M u(s) \\ &= \sum_{i=0}^{\infty} (\sigma_1 G_1 + \cdots + \sigma_{2m} G_{2m})^i B_M u(s), \end{aligned} \tag{11}$$

where $\sigma_i = sp_i - s_0 p_i^0$, $\sigma_{m+i} = p_i - p_i^0$, $G_i = -[s_0 E(p^0) - A(p^0)]^{-1} E_i$, $G_{m+i} = [s_0 E(p^0) - A(p^0)]^{-1} A_i$, $i = 1, 2, \dots, m$, and $B_M = [s_0 E(p^0) - A(p^0)]^{-1} B(p)$, under the condition that all matrices in $[\cdot]^{-1}$ are nonsingular and

$$\|\sigma_1 G_1 + \cdots + \sigma_{2m} G_{2m}\| < 1. \tag{12}$$

Because of condition (12), the resulting ROM is normally accurate only around the expansion point p^0 . To obtain a parametric ROM valid on a wider range, multiple expansion points are often employed as we will show below.

Defining

$$R_j = [G_1, \dots, G_p]R_{j-1}, \quad j = 1, \dots, q,$$

and

$$R_0 = [s_0 E(p^0) - A(p^0)]^{-1} [B_1, \dots, B_m],$$

we can compute the matrix $V_{s_0, p^0, q}$, whose columns form an orthonormal basis of the subspace spanned by the first q of R_i 's:

$$\text{range}\{V_{s_0, p^0, q}\} = \text{span}\{R_0, R_1, \dots, R_q\}_{s_0, p^0}. \tag{13}$$

Using $V := V_{s_0, p^0, q}$, which is assumed to be an $n \times n_r$ matrix, we obtain the parametric reduced-order model via Galerkin projection,

$$\begin{aligned} (V^T E(p)V) \frac{dx_r(t, p)}{dt} &= (V^T A(p)V)x_r(t, p) + (V^T B(p))u(t), \\ y_r(t, p) &= (C(p)V)x_r(t, p) + D(p)u(t), \end{aligned} \tag{14}$$

where the state vector $x_r(t, p)$ is of order n_r . When $A(p), B(p), C(p), E(p)$ all take the affine form (3), the reduced parametric matrices can be computed by the formula

$$\begin{aligned} V^T E(p)V &= p_1 V^T E_1 V + \dots + p_m V^T E_m V, \\ V^T A(p)V &= p_1 V^T A_1 V + \dots + p_m V^T A_m V, \\ V^T B(p) &= p_1 V^T B_1 + \dots + p_m V^T B_m, \\ C(p)V &= p_1 C_1 V + \dots + p_m C_m V, \end{aligned}$$

where all constant matrices on the right-hand side can be pre-computed.

Note that the number of columns in R_j increases exponentially with j . When the number of the parameters in p is larger than 2, or when there are many inputs, multiple expansion points should be used to keep the size of the reduced-order model reasonable. The idea is straightforward. Given a set of expansion points $s_i, p^i, i = 0, \dots, k$ (the superscript i for p is not a power: it only indicates the i -th expansion point), a matrix V_{s_i, p^i} can be computed for each pair (s_i, p^i) as

$$\text{range}\{V_{s_i, p^i, q_r}\} = \text{span}\{R_0, R_1, \dots, R_{q_r}\}_{s_i, p^i}. \tag{15}$$

The final projection matrix V is obtained from the orthogonalization of all matrices V_{s_i, p^i, q_r} ,

$$V = \text{orth}\{V_{s_0, p^0, q_r}, \dots, V_{s_k, p^k, q_r}\}. \tag{16}$$

For similar accuracy, the number q_r in (15) can usually be taken much smaller than q in (13) and normally, only a few well-chosen expansion points suffice. For example, 1 or 2 commonly suffices for q_r , while q must be taken a much larger value depending on the problem. The reason is that, using multiple expansion points, the difficulty of the parametric dependence can be tackled by adding new interpolation points, each of which adds only a few columns due to the small q_r , which is much more economical than using a single expansion point, where this difficulty must be treated with the increase of q , each step of which becomes increasingly more expensive. Consequently, the reduced-order model is normally smaller and more accurate on a broader parameter range when multiple expansion points are used.

The choice of the number and locations of the expansion points (s_i, p^i) has an important influence on the efficiency of multi-moment-matching PMOR methods. Actually, good accuracy and compactness of the reduced-order model can only be achieved when the expansion points are selected judiciously.

In the next section, we introduce a technique for adaptively selecting the expansion points according to an *a posteriori* error bound $\Delta(s, p)$ for the ROM. By using the error bound to access the reliability of the reduced-order model, we develop an automatic procedure for constructing the ROM.

4 Adaptively selecting the expansion points

For the general system (4) with l_I inputs and l_O outputs, the error bound $\Delta(s, p)$ is defined as

$$\Delta(s, p) = \max_{\substack{1 \leq i \leq l_I, \\ 1 \leq j \leq l_O}} \Delta_{ij}(s, p),$$

where $\Delta_{ij}(s, p)$ is the error bound for the (i, j) -th entry of the transfer function matrix of the ROM, i.e.,

$$|H_{ij}(s, p) - \hat{H}_{ij}(s, p)| \leq \Delta_{ij}(s, p),$$

where $H(s, p)$ and $\hat{H}(s, p)$ represent the transfer functions of the full-order model and the reduced-order model, respectively. In this paper, we define the $\Delta_{ij}(s, p)$ as in [3], which is inspired by the *a posteriori* error bounds proposed for the reduced basis method [6]:

$$\Delta_{ij}(s, p) = \frac{\|r_i^{du}(s, p)\|_2 \|r_j^{pr}(s, p)\|_2}{\beta(s, p)} + |(\hat{x}^{du})^* r_j^{pr}(s, p)|,$$

where

$$\begin{aligned} r_j^{pr}(s, p) &= B(:, j) - [sE - A]\hat{x}_j^{pr}, \\ \hat{x}_j^{pr} &= V(sV^T E V - V^T A V)^{-1} V^T B(:, j), \\ r_i^{du}(s, p) &= -C(i, :)^T - [\bar{s}E^T - A^T]\hat{x}_i^{du}, \end{aligned}$$

\bar{s} is the conjugate of s , and the state x_i^{du} of the dual system is approximated by

$$\hat{x}_i^{du} = -V^{du} (\bar{s}(V^{du})^T E^T V^{du} - (V^{du})^T A^T V^{du})^{-1} (V^{du})^T C(i, :)^T.$$

Here, for ease of notation, p is dropped from the matrices $E(p), A(p), B(p)$ and $C(p)$, and the j -th column of $B(p)$ and the i -th row of $C(p)$ are denoted by $B(:, j)$ and $C(i, :)$, respectively. The variable $\beta(s, p)$ is the smallest singular value of the matrix $sE(p) - A(p)$. The matrix V^{du} can be computed, for example, using (15) and (16), but replacing R_0, \dots, R_{q_r} with $R_0^{du}, R_1^{du}, \dots, R_{q_r}^{du}$, where the matrices $s_i E(p^i) - A(p^i)$ in R_0, \dots, R_{q_r} are substituted by $\bar{s}_i E^T(p^i) - A^T(p^i)$, and E_j by E_j^T , A_j by A_j^T , B_j by $C(j, :)^T$, $j = 1, \dots, m$. The derivation of $\Delta(s, p)$ is detailed in [3].

Algorithm 1 Adaptively selecting expansion points \hat{s}, \hat{p} , and computing V automatically

- 1: $V = []; V^{du} = [];$
 - 2: Choose some $\varepsilon_{\text{tol}} < 1$ and a small positive integer q_r ; set $\varepsilon = 1$;
 - 3: Choose Ξ_{train} : a large set of samples of s and p , taken over the domain of interest;
 - 4: Choose the initial expansion point: (\hat{s}, \hat{p}) ;
 - 5: **while** $\varepsilon > \varepsilon_{\text{tol}}$ **do**
 - 6: $\text{range}(V_{\hat{s}, \hat{p}, q_r}) = \text{span}\{R_0, R_1, \dots, R_{q_r}\}_{\hat{s}, \hat{p}};$
 - 7: $\text{range}(V_{\hat{s}, \hat{p}, q_r}^{du}) = \text{span}\{R_0^{du}, R_1^{du}, \dots, R_{q_r}^{du}\}_{\hat{s}, \hat{p}};$
 - 8: $V = \text{orth}\{V, V_{\hat{s}, \hat{p}, q_r}\};$
 - 9: $V^{du} = \text{orth}\{V^{du}, V_{\hat{s}, \hat{p}, q_r}^{du}\};$
 - 10: $(\hat{s}, \hat{p}) = \arg \max_{s, p \in \Xi_{\text{train}}} \Delta(s, p);$
 - 11: $\varepsilon = \Delta(\hat{s}, \hat{p});$
 - 12: **end while.**
-

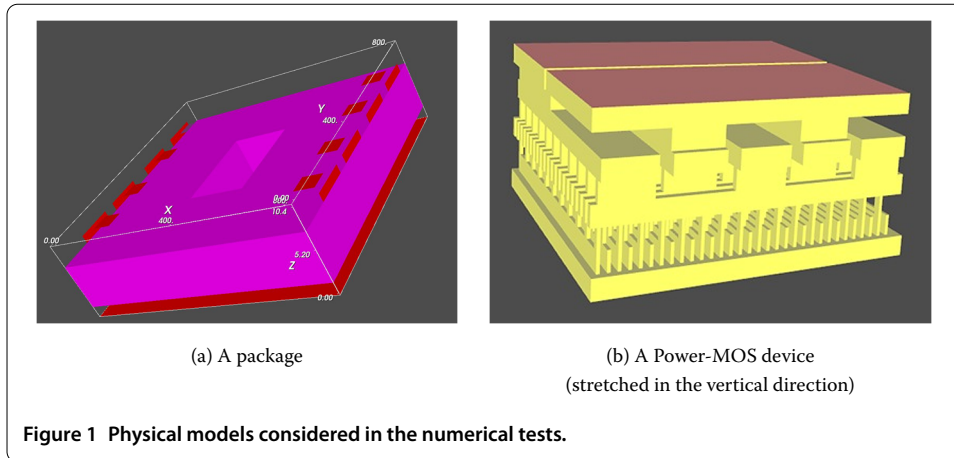
Thanks to the error bound $\Delta(s, p)$ for the ROM, the expansion points (s_i, p^i) can be selected adaptively, and the projection matrix V can be computed automatically as is shown in Algorithm 1. It is worth pointing out that although the error bound is parameter-dependent, many p -independent terms constituting the error bound need to be pre-computed only once, which can be repeatedly used in the algorithm for all samples of p in Ξ_{train} , e.g., the terms $V^T M_1 V, \dots, V^T M_m V$, etc.

5 Test models

To test the techniques proposed, we will use two applications arising from thermal and electro-thermal simulations: a package shown in Figure 1(a), whose purpose is to allow easy handling and assembly onto printed circuit boards and to protect the devices from damage [7], and a Power-MOS device shown in Figure 1(b), which is commonly used in energy harvesting, where energy from external sources like light and environmental heat is collected in order to power small devices such as implanted biosensors [8, 9]. With the scaling down of integrated circuits, thermal issues have attracted increasingly more attentions and become a major consideration in the design of integrated circuits.

The dynamics of both applications can be described by the same governing equations. The electrical sub-system can be described by

$$\begin{aligned} \nabla \cdot J + \frac{\partial \rho}{\partial t} &= 0, \\ J &= \sigma \cdot E, \quad E = -\nabla U, \\ \rho &= -\nabla \cdot (\epsilon \nabla U), \end{aligned}$$



where J is the current density, E is the electrical field, U is the electrical potential, σ is the electrical conductivity, ϵ is the permittivity, and ρ is the charge density. In this paper, we ignore both the local charging, i.e., $\epsilon = 0$ and $\rho = 0$, and the dependence of the electrical conductivity σ on temperature, i.e., the electrical sub-system is independent of the thermal sub-system, and obtain the following simplified governing differential equation, which is time-independent:

$$\nabla \cdot (\sigma \cdot \nabla U) = 0.$$

The thermal sub-system is governed by similar equations:

$$\nabla \cdot \phi_q + \frac{\partial w(T)}{\partial t} = Q,$$

$$\phi_q = -\kappa \nabla T,$$

$$w(T) = C_T(T - T_{\text{ref}}),$$

where ϕ_q is the heat flux, w is the local energy storage, C_T is the thermal capacitance, and Q represents heat sources or sinks. For the thermal sub-system, we also ignore the dependence of the thermal capacitance on the temperature. For Q , we use two options in this paper.

- The thermal-only option takes Q as an independent input. Under this option, the electrical sub-system and the thermal sub-system are completely decoupled. The thermal-only option is especially interesting to the package model, since it can be used to study the thermal dynamics stimulated by heat-injecting or extracting properties on the boundary of the simulation domain, Joule self-heating, etc. Finite element discretization of the thermal-only option leads to a linear dynamical system exactly the form (2).

- The electro-thermal option takes Q as a coupling term from the electrical sub-system: the Joule self-heating that is of great importance in power-aware design of integrated circuits:

$$Q = Q_{\text{SH}} = E \cdot J.$$

In this case, the whole system is one-way coupled: the thermal sub-system depends on the electrical sub-system, while the electrical sub-system is independent of the thermal system. The state space representation of the electro-thermal option is:

$$\begin{cases} A_E(p)x_E(t,p) = -B_E(p)u(t), & (17a) \\ E_T(p)\dot{x}_T(t,p) = A_T(p)x_T(t,p) + B_T(p)u(t) + F(p) \times_2 x_E(p) \times_3 x_E(p), & (17b) \\ x_T(0,p) = x_T^0, \quad x_E(0,p) = x_E^0, & (17c) \\ y(t,p) = C_E(p)x_E(t,p) + C_T(p)x_T(t,p) + D(p)u(t), & (17d) \end{cases}$$

where the input vector $u \in \mathbb{R}^{l_i}$ represents the input voltages and temperatures at the contacts, the output vector $y \in \mathbb{R}^{l_o}$ represents the output voltages, currents, temperature, and thermal fluxes at the contacts, $A_E(p) \in \mathbb{R}^{n_E \times n_E}$, $B_E(p) \in \mathbb{R}^{n_E \times l_i}$, $E_T(p) \in \mathbb{R}^{n_T \times n_T}$, $A_T(p) \in \mathbb{R}^{n_T \times n_T}$, $B_T(p) \in \mathbb{R}^{n_T \times l_i}$, $C_E(p) \in \mathbb{R}^{l_o \times n_E}$, $C_T(p) \in \mathbb{R}^{l_o \times n_T}$, $D_T(p) \in \mathbb{R}^{l_o \times l_i}$, and the tensor $F(p) \in \mathbb{R}^{n_T \times n_E \times n_E}$, which can be considered as n_T slices of n_E by n_E matrices $F_i(p) \in \mathbb{R}^{n_E \times n_E}$, $i = 1, \dots, n_T$, represents the nonlinear coupling of the electrical part with the thermal part. Denoting the i -mode tensor-matrix product by \times_i [10], the product $F(p) \times_2 x_E(p) \times_3 x_E(p)$ is a vector of length n_T , whose i -th component is the standard vector-matrix-vector product $x_E(p)^T F_i(p) x_E(p)$. In this formulation, the algebraic equation (17a) describes the electrical part, the ordinary differential equation (17b) describes the thermal part, in which the tensor $F(p)$ describes Joule self-heating, (17c) specifies the initial conditions, and (17d) computes the output obtained from the electrical and thermal state vectors. Theoretically, Joule self-heating should be modeled by two tensor products: $F(p) \times_2 x_E(p) \times_3 x_E(p)$ and $G(p) \times_2 x_E(p) \times_3 u(t)$. However, the influence of the second part is rather limited, and is therefore ignored in this paper. Instead of a single coupled system, we write out the electrical and thermal sub-systems explicitly to show the one-way coupling. Furthermore, our numerical results proved that PMOR is computationally much more efficient if we apply it to the algebraic equations and the ordinary differential equations separately rather than apply it to a single set of differential algebraic equations.

6 Parametric modeling and PMOR for the test models

For the package model shown in Figure 1(a), the parameter p is chosen to be the top layer thickness of the package, namely h . The finite-integration technique (FIT) for the modeling of the package leads to thermal fluxes that are proportional to the dual areas of the mesh cells and inversely proportional to the lengths of the edges in the mesh cells. Therefore, when considering meshes that are topologically equivalent for different package thicknesses, the parametric dependence of the matrices will take the form

$$M(h) = M_0 + hM_1 + \frac{1}{h}M_2 \quad (M = A_E, B_E, E_T, A_T, B_T, F, C_E, C_T, D).$$

The second term originates from the linear dependence of dual areas corresponding to the cell edges perpendicular to the thickness orientation, whereas the third term originates from dual areas associated to cell edges tangential to the thickness orientation [11]. It is clear that the above formulation is a special case of (3) with $p_1 = 1$, $p_2 = h$, and $p_3 = \frac{1}{h}$.

Note that the method developed in Section 2 also applies to the tensor F due to the following reasoning. Every slice of F , say $F_i(p) \in \mathbb{R}^{n_E \times n_E}$, can be extracted using the procedure from (6) to (8), and under the same set of samples $p^{a_1}, p^{a_2}, \dots, p^{a_m}$ in (6), the obtained coefficients $\tilde{p}_{11}, \tilde{p}_{12}, \dots, \tilde{p}_{mm}$ in (8) are the same. Therefore, the computation for all slices can be conducted together in the tensor form, i.e., assuming that M_1, M_2, \dots, M_m in (6) are tensors, they can be extracted by (8), using the coefficient computed by (9).

Therefore, to extract all matrices and tensors for the package model, we need first only to invert a single 3×3 matrix, and then, for each matrix or tensor function, we need to calculate (8) once.

For the Power-MOS circuit model shown in Figure 1(b), the conductivity of the third metal layer, which we denote by σ , is chosen to be the parameter. The finite-integration technique (FIT) assembles fluxes that are proportional to the conductivity of each mesh cell material, and therefore, the parametric dependence of the matrices will take the form

$$M(\sigma) = M_0 + \sigma M_1 \quad (M = A_E, B_E, E_T, A_T, B_T, F, C_E, C_T, D).$$

It is clearly in the form (3) by assigning $p_1 = 1$ and $p_2 = \sigma$, and the proposed procedure for extracting the matrices/tensors can readily be used.

The remaining problem is how to reduce system (17b), which has a quadratic one-way coupling term. To simplify the presentation, we use the Power-MOS circuit with the parameter dependence $M(\sigma) = M_0 + \sigma M_1$ as an example. Following the idea presented in [12], we first ignore the nonlinear part $F(p) \times_2 x_E(p) \times_3 x_E(p)$ in system (17b) and use the adaptive PMOR algorithm proposed to reduce the resulting system in the form (4) [7, 9]. To approximate the one-way coupling term, we need to reduce the electrical sub-system before the thermal sub-system.

- The electrical sub-system (17a) is already in the form (10) if we assign $E(p) = 0, A(p) = -A_E(p), B(p) = -B_E(p), s = t$, by noting that for the validity of the proposed PMOR method, system (10) is actually not necessarily a frequency-domain system. Denote the basis built for the electrical sub-system (17a) by V_E . For MOR for algebraic equations, it is worth mentioning the exact reduction method proposed in [13] for non-parametric systems, which does not require an error bound. However, the method we propose in this paper can not only reduce parametric systems, but also normally build a reduced-order model of a much lower dimension.

- If we ignore the nonlinear coupling term in the thermal sub-system (17b), it is already in the form (4). To use the methods developed, we first conduct the Laplace transform to obtain its frequency domain representation

$$(A_{T1} + \sigma A_{T2} - sE_{T1} - (\sigma s)E_{T2})X = [B_{T1} B_{T2} A_{T1} x_T^0 A_{T2} x_T^0] \begin{bmatrix} -U \\ -\sigma U \\ \frac{-1}{s} \\ \frac{-\sigma}{s} \end{bmatrix}. \tag{18}$$

Then, we apply Algorithm 1 to system (18) to obtain the basis for the thermal sub-system, which we denote by V_T .

- To obtain a ROM for (17b), we approximate x_E by $V_E \hat{x}_E$ and x_T by $V_T \hat{x}_T$, and then force the approximation error to be orthogonal to the range of V_T . The resulting parametric

ROM is

$$\widehat{E}_T(p)\widehat{x}_T(t,p) = \widehat{A}_T(p)\widehat{x}_T(t,p) + \widehat{B}_T(p)u + \widehat{F}(p) \times_2 \widehat{x}_E(p) \times_3 \widehat{x}_E(p), \tag{19}$$

where $\widehat{E}_T(p) = V_T^T E_T(p) V_T$, $\widehat{A}_T(p) = V_T^T A_T(p) V_T$, $\widehat{B}_T(p) = V_T^T B_T(p)$, $\widehat{F}(p) = F(p) \times_1 V_T \times_2 V_E \times_3 V_E$. To obtain the reduced tensor $\widehat{F}(p)$, we first approximate $x_E(p)$ in the range of V_E , and then project the approximation onto the test subspace V_T , i.e., the tensor product $\widehat{F}(p) \times_2 \widehat{x}_E(p) \times_3 \widehat{x}_E(p)$ equals $V_T^T [F(p) \times_2 (V_E \widehat{x}_E(p)) \times_3 (V_E \widehat{x}_E(p))]$. The advantage of the tensor formulation for the ROM is that using the reduced tensor, evaluating the ROM does not require computations with quantities of the order of the FOM. In our actual computations, the parametric matrices in the ROM are computed by

$$\widehat{Y}(p) = \widehat{Y}_c + p\widehat{Y}_v, \quad \widehat{Y} \in \{\widehat{A}_T, \widehat{B}_T, \widehat{C}_T, \widehat{E}_T, \widehat{F}\}, \tag{20}$$

where \widehat{Y}_c and \widehat{Y}_v are pre-computed during the construction of the ROM. This precomputation is also applied to the electrical sub-system (17a) and the output computation (17d).

7 Numerical results

In this section, we first show the numerical results of the thermal analysis of the package model. Then, we present the numerical results of the electro-thermal analysis of both the package model and the Power-MOS device model.

7.1 Numerical results for the thermal analysis

The package model is a multi-input multi-output system, with 34 inputs and 68 outputs. Algorithm 1 is employed to compute the parametric reduced-order model automatically. We used 6 samples of the package thickness $h \in (0 \mu\text{m}, 100 \mu\text{m}]$, and one sample of $s = 2\pi f J$, $f \in [0 \text{ Hz}, 10^8 \text{ Hz}]$: $s_0 = 200\pi J$, $J = \sqrt{-1}$, to constitute the training set Ξ_{train} in Algorithm 1. The algorithm essentially selects the expansion points for p , since we fix s to the single expansion point s_0 . Only two iterations and two expansion points selected are required for convergence. The reduced-order model is of size $r = 58$. For each selected expansion point, we construct V_{s_i,p^i} with only two terms R_0 and R_1 ($q_r = 1$ in Steps 6-7, Algorithm 1) in order to avoid the exponential increase in R_j , $j > 1$. Table 1 lists the iterations and the error bounds at each iteration step.

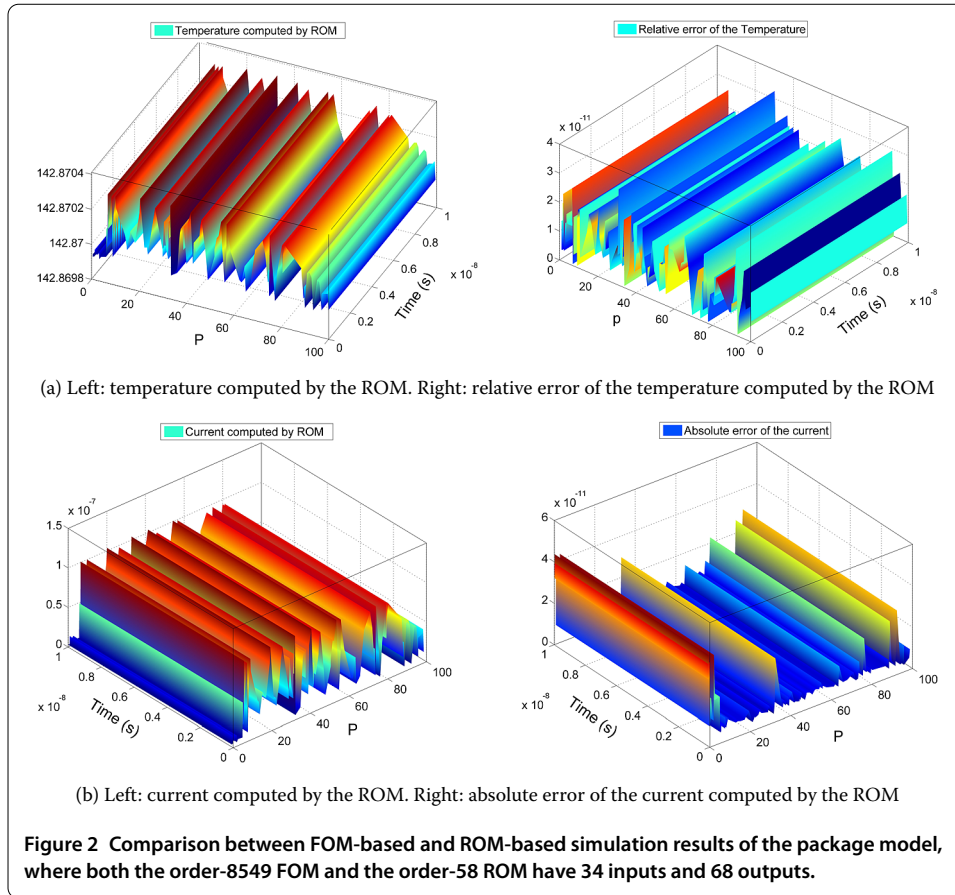
Figure 2(a) and (b) plot the temperature and the current at two different parts of the package, respectively. The temperature is of big magnitude, while the current is of very small magnitude, showing that there is no current at that part of the circuit. The reduced-order model catches the accuracy of both at 120 samples of p , and 100 time steps for each sample.

7.2 Numerical results for the electro-thermal analysis

First, we apply the matrix extraction algorithm and adaptive PMOR method developed to the electro-thermal simulation of the package model with 34 inputs and 68 outputs.

Table 1 $V_{s_i,p^i} = \text{span}\{R_0, R_1\}_{s_i,p^i}$, $i = 1, 2$, $\epsilon_{\text{tol}} = 10^{-3}$, $n = 8,549$, $r = 58$

Iteration i	(s_0, h^i)	$\Delta(s_0, h^i)$
1	$(200\pi J, 0.3834)$	0.0153
2	$(200\pi J, 0.0677)$	5×10^{-4}



The system is parameterized by the thickness of the top layer and excited by the inputs:

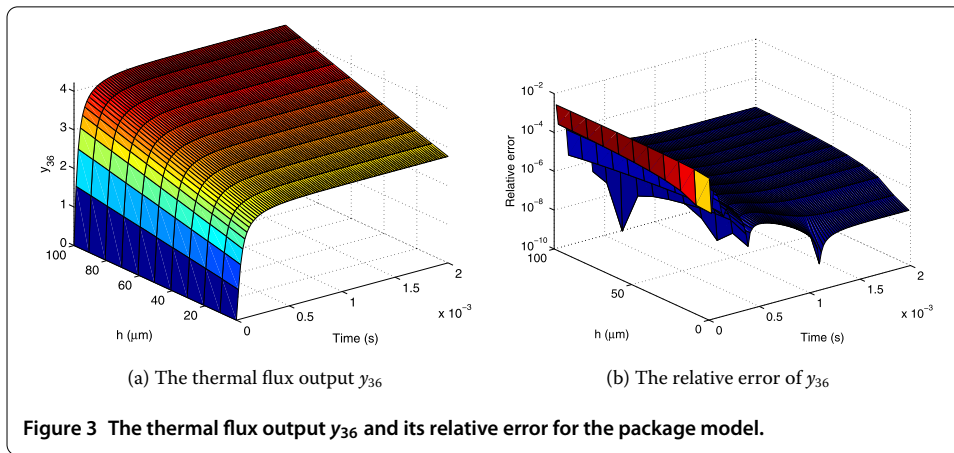
$$u_i = \begin{cases} 1, & i = 1, \\ 0, & 2 \leq i \leq 17, \\ 75 \times 10^8 t + 75, & i = 18, t \in [0, 10^{-8}], \\ 150 & i = 18, t > 10^{-8}, \\ 75 & 19 \leq i \leq 34. \end{cases}$$

The initial condition for all electrical state variables is 0 V, and the initial condition for all thermal state variables is 75°C. For the electrical sub-system, the training set is {1, 2, 5, 8, 10, 20, 30, 40, 50, 60, 70, 80, 90, 100} (in μm), while for the thermal sub-system, the training set {(s, h)} contains 20 samples, in which the frequency (s) and the thickness of the top metal layer (h) are uniformly chosen within the ranges [0 rad/s, 100 rad/s] and (0 μm, 30 μm], respectively. Using the PMOR method proposed, the electrical sub-system is reduced from order 1,122 to order 68, the thermal system is reduced from order 8,071 to order 606, and the speedup factor for the electro-thermal simulation is 7.2. The convergence behavior of the adaptive PMOR method is shown in Table 2 and the thermal flux output y_{36} and its relative error are shown in Figure 3.

Then, we apply the proposed methods to the Power-MOS circuit model, which has 6 inputs and 12 outputs. The system is parameterized by the conductivity of the third metal

Table 2 Convergence behavior of electro-thermal simulation of the package model ($\epsilon_{\text{tol}} = 10^{-4}$)

Iteration	Electrical sub-system		Thermal sub-system	
	Selected sample h	Error bound	Selected sample (s, h)	Error bound
1	1	2.1×10^3	(8.1339, 7.5910)	7.3×10^6
2	100	3.7×10^0	(41.065, 29.653)	2.3×10^1
3	90	6.6×10^{-2}	(17.494, 15.121)	1.3×10^{-1}
4	80	6.4×10^{-3}	(16.455, 4.6942)	7.8×10^{-5}
5	70	5.3×10^{-3}	–	–
6	60	4.2×10^{-3}	–	–
7	50	3.1×10^{-3}	–	–
8	40	1.8×10^{-3}	–	–
9	30	8.9×10^{-4}	–	–



layer and excited by the inputs:

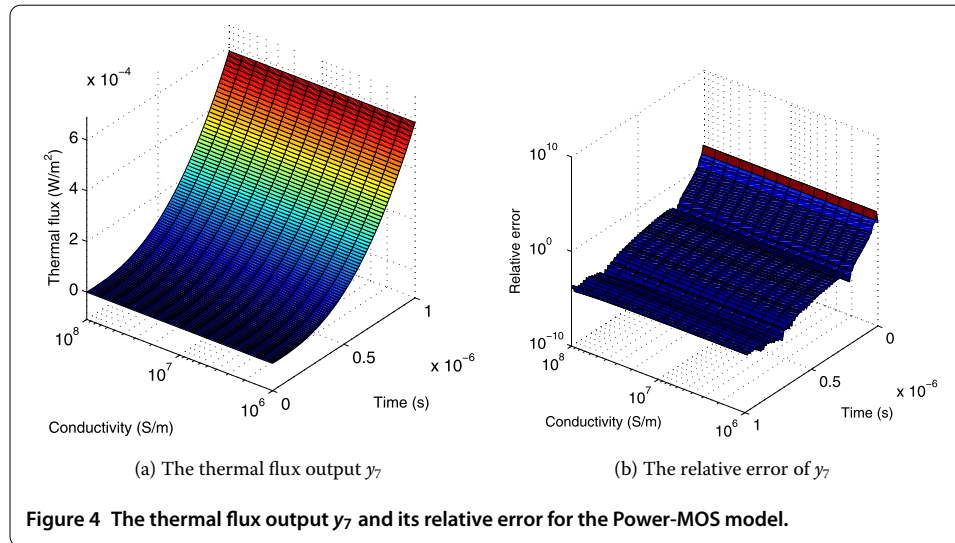
$$u_i = \begin{cases} 0, & i = 1, 2, \\ 10^7 t, & i = 3, t \in [0, 10^{-6}], \\ 10, & i = 3, t > 10^{-6}, \\ 26.85, & i = 4, 5, 6. \end{cases}$$

The initial condition for all electrical state variables is 0 V, and the initial condition for all thermal state variables is 26.85 °C. For the electrical sub-system, the training set is $\{10^7 \text{ S/m}, 3 \times 10^7 \text{ S/m}, 5 \times 10^7 \text{ S/m}\}$, while for the thermal sub-system, the training set $\{(s, \sigma)\}$ contains 20 samples, in which the frequency (s) and the conductivity of the top metal layer (σ) are uniformly chosen within the ranges $[0 \text{ rad/s}, 10^6 \text{ rad/s}]$ and $[10^7 \text{ S/m}, 5 \times 10^7 \text{ S/m}]$, respectively. Using the PMOR methods proposed, the electrical sub-system is reduced from order 1,160 to order 2, the thermal sub-system is reduced from order 11,556 to order 35, and the speedup factor for the electro-thermal simulation is 65.93. The convergence behavior of the adaptive PMOR method is shown in Table 3 and the thermal flux output y_7 along with its relative error is shown Figure 4.

Figure 4(b) shows that the relative error is large when t is small, e.g., with a value in the range of $[10, 100]$ at the time 10^{-9} s. The reason is that the thermal flux is still very close to zero (the circuit is hardly heated up) and the numerical error arising from the discretization of the FOM results in numerical noise, which dominates the output of the

Table 3 Convergence behavior of electro-thermal simulation of the Power-MOS model ($\epsilon_{\text{tol}} = 10^{-12}$)

Iteration	Electrical sub-system		Thermal sub-system	
	Selected sample σ	Error bound	Selected sample (s, σ)	Error bound
1	10^7	7.165399×10^{-24}	$(0, 2.736 \times 10^7)$	43.73
2	–	–	$(10^6, 2.537 \times 10^7)$	4.225×10^{-4}
3	–	–	$(2.632 \times 10^5, 1.694 \times 10^7)$	4.345×10^{-8}
4	–	–	$(5.790 \times 10^5, 2.687 \times 10^7)$	9.774×10^{-11}
5	–	–	$(5.263 \times 10^4, 2.836 \times 10^7)$	4.041×10^{-13}



FOM when the true physical dynamics is small. As Figure 4(b) shows, the ROM approximates the thermal flux accurately after the thermal flux dominates the numerical error ($t > 2 \times 10^{-7}$). Therefore, the ROM can not only approximate the true dynamics accurately, but is also robust to the numerical error present in the FOM due to discretization. Furthermore, although the samples are selected within the range $[10^7, 5 \times 10^7]$, Figure 4(b) shows that the parametric ROM is valid in a much wider range.

8 Conclusions and further discussion

We have proposed a simple automatic matrix extracting technique for a class of parametric dynamical systems, and shown that automatic parametric model order reduction can be realized with the guidance of an *a posteriori* error bound. The above techniques have been successfully applied to the thermal simulation of a package model, and the electro-thermal simulation of a package model and a Power-MOS device model. Compact and reliable reduced-order models have been automatically obtained, which offers the possibility of being integrated into dedicated electro-thermal simulation software to accelerate design automation.

It is worth pointing out that although the adaptive Algorithm 1 for multi-moment-matching PMOR methods resembles the greedy algorithm that is often used in the reduced basis method [6], the size of the training sets we used in numerical tests, which is 20 in all three examples, is much smaller than that typically used in reduced basis methods, which can easily reach 1,000 or even 10,000. Numerical simulations show that this small

number of training points leads to accurate ROMs within a large parameter range. Another phenomenon we observed in numerical tests for electro-thermal analysis is that the resulting parametric ROMs are robust to numerical error introduced by PDE discretization.

Competing interests

The authors declare that they have no competing interests.

Authors' contributions

The main idea of the paper was proposed by LF. The numerical simulations were mainly done by LF, YY and NB. The manuscript was initially prepared by YY. PB did thorough correction of the manuscript. Authors from MAGWEL provided the data (models, matrices) for numerical tests. All authors read and approved the final manuscript.

Author details

¹Max Planck Institute for Dynamics of Complex Technical Systems, Sandtorstr. 1, Magdeburg, 39106, Germany. ²Magwel NV, Martelarenplein 13, Leuven, 3000, Belgium.

Acknowledgements

This work is financially supported by the collaborative project nanoCOPS [14], Nanoelectronic COupled Problems Solutions, supported by the European Union in the FP7-ICT-2013-11 Program under Grant Agreement Number 619166.

Received: 14 February 2016 Accepted: 18 October 2016 Published online: 08 November 2016

References

1. Benner P, Gugercin S, Willcox K. A survey of projection-based model reduction methods for parametric dynamical systems. *SIAM Rev.* 2015;57(4):483-531.
2. Benner P, Feng L. A robust algorithm for parametric model order reduction based on implicit moment matching. In: Quarteroni A, Rozza G, editors. *Reduced order methods for modeling and computational reduction. MS&A - modeling, simulation and applications.* vol. 9. Heidelberg: Springer; 2014. p. 159-85.
3. Feng L, Antoulas AC, Benner P. Some a posteriori error bounds for reduced order modelling of (non-)parametrized linear systems. Max Planck Institute Magdeburg Preprint MPIMD/15-17, MPI-Magdeburg; 2015. Available from <http://www.mpi-magdeburg.mpg.de/preprints/>.
4. Barrault M, Maday Y, Nguyen NC, Patera AT. An 'empirical interpolation' method: application to efficient reduced-basis discretization of partial differential equations. *C R Math.* 2004;339(9):667-72. doi:10.1016/j.crma.2004.08.006.
5. Horn RA, Johnson CR. *Topics in matrix analysis.* Cambridge: Cambridge University Press; 1991.
6. Rozza G, Huynh DBP, Patera AT. Reduced basis approximation and a posteriori error estimation for affinely parametrized elliptic coercive partial differential equations. *Arch Comput Methods Eng.* 2007;15(3):229-75.
7. Banagaaya N, Feng L, Meuris P, Schoenmaker W, Benner P. Model order reduction of an electro-thermal package model. *IFAC-PapersOnLine.* 2015;48(1):934-5. Presented at the 8th Vienna International Conference Mathematical Modelling - MATHMOD2015.
8. Spirito P, Breglio G, d'Alessandro V, Rinaldi N. Thermal instabilities in high current power MOS devices: experimental evidence, electro-thermal simulations and analytical modeling. In: *23rd International Conference on Microelectronics. MIEL.* vol. 1. 2002. p. 23-30. doi:10.1109/MIEL.2002.1003144.
9. Yue Y, Feng L, Meuris P, Schoenmaker W, Benner P. Application of Krylov-type parametric model order reduction in efficient uncertainty quantification of electro-thermal circuit models. In: *PIERS Proceedings.* Prague. 2015. p. 379-84.
10. Kolda TG, Bader BW. Tensor decompositions and applications. *SIAM Rev.* 2009;51(3):455-500.
11. Benner P, Feng L, Schoenmaker W, Meuris P. Parametric modeling and model order reduction of coupled problems. *ECMI Newsl.* 2014;56:68-9.
12. Chen Y. *Model order reduction for nonlinear systems.* Master's thesis. Massachusetts Institute of Technology; 1999.
13. Rommes J, Schilders WHA. Efficient methods for large resistor networks. *IEEE Trans Comput-Aided Des Integr Circuits Syst.* 2010;29(1):28-39. doi:10.1109/TCAD.2009.2034402.
14. ter Maten EJW, Putek PA, Günther M, Pulch R, Tischendorf C, Strohm C, Schoenmaker W, Meuris P, De Smedt B, Benner P, Feng L, Banagaaya N, Yue Y, Janssen R, Dohmen JJ, Tasić B, Deleu F, Gillon R, Wieers A, Brachtendorf H-G, Kratochvíl T, Petřizela J, Sotner R, Götthans T, Dřínovský J, Schöps S, Duque Guerra DJ, Casper T, De Gersem H, Römer U, Reynier P, Barroul P, Masliah D, Rousseau B. Nanoelectronic COupled problems solutions - nanoCOPS: modelling, multirate, model order reduction, uncertainty quantification, fast fault simulation. *J Math Ind.* 2016;7:2. doi:10.1186/s13362-016-0025-5